# Relaxation on critical percolation clusters, self-avoiding random walks, and the quantum Hall effect

F. Evers
*Department of Physics and Materials Science Institute, University of Oregon, Eugene, Oregon 97403*
(Received 2 October 1996)

Large contour lines in a random landscape constitute a continuum percolation problem. We consider directed walks on these lines at the percolation threshold—self-avoiding by construction—and calculate the density correlation function using a Monte Carlo simulation. It has a scaling structure where all exponents are related to the fractal dimension $d_h=7/4$ of extended contour lines. The corresponding scaling function, however, *vanishes* in the limit $\omega\to 0$ with a power law giving rise to another *a priori* independent exponent $\zeta$. Our data indicate a Cole-Cole structure for the quantity $\chi''(\boldsymbol{\omega})$ averaged over extended lines only, which implies $\zeta=2/7$, $\eta=0$ and an anomaly in the small frequency asymptotics of the diffusion coefficient $D(\boldsymbol{q},\omega)\propto\omega^{-\zeta}/q^2$. This anomaly is reminiscent of a similar one in the quantum Hall effect, however, with negative $\zeta_{qhe}$. We argue that the difference is due to the decay of phase resonances in the latter which come with a broad distribution of decay times. [S1063-651X(97)14102-2]

PACS number(s): 64.60.Ak, 71.30.+h, 73.40.Hm

## I. INTRODUCTION

Contour lines in a random but smooth landscape constitute a typical continuum percolation problem [1]. The lines are all closed at very low elevation. With increasing altitude the mean extension of the contour lines grows until finally there is a line spanning the entire landscape so that it becomes percolating.

One can attribute an orientation and a velocity to an ant moving on such a contour line: If it walks around an island it moves clockwise, otherwise counterclockwise. Its speed is proportional to the mountains slope at its position. As contour lines never intersect, the ant—from its own point of view—behaves as if performing a particular type of self-avoiding random walk. It is in the same universality class as the ''smart kinetic walk'' introduced earlier by Weinrib and Trugman [2].

This model—extended by the semiclassical quantization condition of integer flux between two neighboring contour lines—is an accurate description for the propagation of electrons in the semiclassical, high magnetic field limit [3]. In the context of the Integer quantum Hall effect it provides an intuitive approach to the experimental facts [4].

Its predictions for the critical exponents in actual quantum Hall systems are incorrect, however (e.g., $\nu_p=4/3$ instead of $\nu_{qhe}=2.3\pm 0.1$ [5]). Nevertheless, in a previous study [6] we have found that the result for the dynamical conductivity at criticallity coincides with the numerical results of full quantum mechanical calculations [7,8]. In particular, we have recovered the supposed to be universal value for the static conductivity $\sigma_{xx}=0.5\pm 0.02e^2/h$ and the ''long time tail'' anomaly.

In these calculations we have seen that it is essential to distinguish two different kinds of averages over ant trajectories: one average takes only such paths into account which do not close within the observation time; whereas another procedure counts all orbits regardless if they are closing or not. Ant motion on open trajectories is superdiffusive in the sense that the mean square deviation from the origin increases, like $t^{1+\delta}$, where $\delta=1/7$ is positive. Here $\delta$ can easily be traced back to the fractal dimension of the hull. The latter describes the relation

$$R^{d_h}\propto L \tag{1}$$

of the extension of a trajectory to its length. Given that the average velocity of an ant may be taken as constant, we derive $\delta=2/d_{\mathrm{h}}-1=1/7$.

However, to obtain a prediction for the experimentally relevant conductivity one actually has to average over *all* contour lines. We have demonstrated analytically and by means of a numerical simulation that one obtains a simple diffusion law in this case. All analytical considerations heavily make use of the analogy to the site percolation theory, by assuming that contour lines have the same statistical properies as cluster hulls. This assumption, however, is established very well [9,10].

In this paper we extend our previous work and analyze the wave number dependence of the density correlation function by means of a Monte Carlo simulation of ant tracks in random mountains. More specifically the object of investigation is the structure factor $S(\boldsymbol{q},\omega)$ which is related to the spectral function as $\chi''(\boldsymbol{q},\omega)=\omega S(\boldsymbol{q},\omega)/2$. Averaging all contour lines we find the scaling structure

$$S(\boldsymbol{q},\omega)=q^{-2+\hat{\eta}}\theta(\omega/q^z),\quad z=7/4,\ \hat{\eta}=1/2 \tag{2}$$

where all exponents can be related to the fractal dimension of the hull $d_h=7/4$. From the scaling point of view the long time tail anomaly in the $q=0$ conductivity is a correction to scaling.

It turns out, that the scaling function $\theta(x)$ itself provides another exponent $\zeta=0.28\pm 0.05$ because it *vanishes* in the limit of small arguments with a power law. As a consequence the conventional exponent $\eta$ describing the wave number dependence of the density correlation function in the limit of vanishing frequency and $\hat{\eta}$ are not identical and

 

instead $\eta=\hat{\eta}-\zeta z$. Our numerical results suggest that $\eta=0$. This is consistent with a Cole-Cole form of $\chi''(\omega)$ for the quantity averaged over extended orbits. The corresponding exponent $\alpha=8/7$, however, is larger than unity opposed to the usual case [11] where $\alpha\leqslant 1$. The anomaly in the scaling function leads to a power law for the diffusion coefficient at small frequencies

$$D(\boldsymbol{q},\omega)\propto\omega^{-\zeta}/q^2,\quad \omega/q^z\ll 1.$$

One can modify the current model by allowing ants to hop across saddle points with a certain probability. We still observe an anomalous diffusion coefficient, however, with a negative exponent $\zeta$. We discuss the connection to a similar power law anomaly in the quantum Hall effect.

## II. THE CONTINUUM MODEL

For calculating the ant paths we use a model which was described in detail in an earlier publication [6]. Here we just give a brief summary on how it works.

Per definition, our model on ant dynamics can be represented by the equations of motion

$$\dot{x}=\frac{\partial V}{\partial y},\qquad \dot{y}=-\frac{\partial V}{\partial x}. \tag{3}$$

Here $(x,y)$ denotes the ant's position, while $V(\boldsymbol{r})$ its elevation in a random landscape. We take $V(\boldsymbol{r})$ to be a superposition of Gaussians placed on a square lattice

$$V(\boldsymbol{r})=\sum_{i,j} a_{i,j}\exp\left(\frac{-|\boldsymbol{r}-\boldsymbol{r}_{ij}|^2}{4}\right). \tag{4}$$

Our procedure for obtaining an ant path $\boldsymbol{r}(t)$ goes as follows: First we pick the amplitudes $a_{i,j}$ at random from the interval $[-1,1]$. Then we choose a point $\boldsymbol{r}(0)$ in the landscape such that $V[\boldsymbol{r}(0)]=0$ being the critical elevation in our model. Starting out from here we integrate the equations of motion (3) numerically.

These equations faithfully describe ant movements on the microscopic scale. In this context it has been argued [12] that the slowing down of the ant near saddle points has substantial influence on its long time dynamics: On an infinitely extended trajectory it will finally come so close to a saddle point that it asymptotically stops. However, in our calculations we did not observe this slowing down. As outlined in Appendix B, the above mentioned argument neglects how the probability of coming close to a saddle point increases with the walking distance. It turns out, that the increase is much too weak to reduce the average velocity on very long contour lines substantially.

## III. SIMULATION RESULTS

We discuss the outcome for the relaxation function first.

$$F(\boldsymbol{q},t)=\langle\cos\{\boldsymbol{q}[\boldsymbol{r}(t)-\boldsymbol{r}(0)]\}\rangle. \tag{5}$$

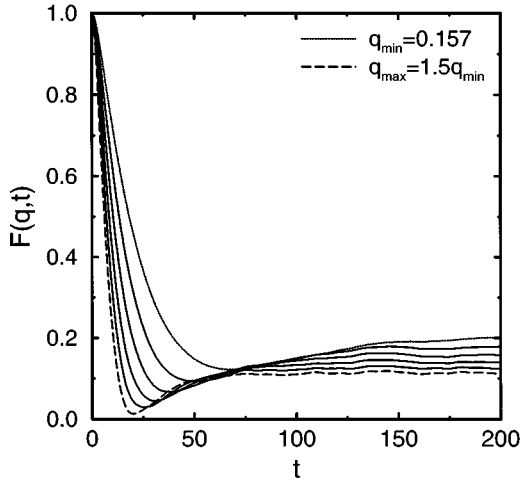


FIG. 1. Relaxation function averaged over all detected trajectories. The unit of time is set by the average time needed to travel one correlation length of the random landscape along a trajectory. The dashed line corresponds to the largest of the six equidistant wave numbers, the uppermost line to the smallest one.

The angular brackets indicate an average over ant paths.

Figures 1 and 2 depict our results for both averages. We restrict our discussion to the total average $F(\boldsymbol{q},t)$ and only mention the analogous features of $F_0(\boldsymbol{q},t)$. We denote open orbit quantities with an index 0.

The continuum model has a microscopic time scale $\tau$ connected with the correlation length of the random potential. For times $t$ being larger than $\tau$, though small enough to allow for an expansion of the ''cosine'' in Eq. (5)

$$F(\boldsymbol{q},t)=1-\tfrac{1}{4}q^2\langle[\boldsymbol{r}(t)-\boldsymbol{r}(0)]^2\rangle+\cdots,$$

the relaxation function is dominated by the $q=0$ diffusion behavior

$$\langle[\boldsymbol{r}(t)-\boldsymbol{r}(0)]^2\rangle=4Dt,\qquad \langle[\boldsymbol{r}(t)-\boldsymbol{r}(0)]^2\rangle_0=4D_0t^{1+\delta}, \tag{6}$$

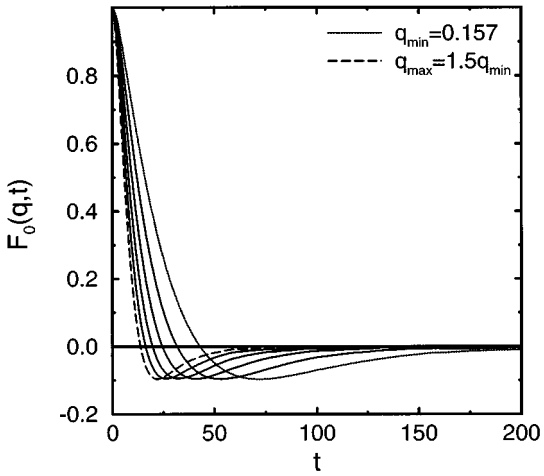


FIG. 2. Relaxation function averaged over orbits which did not close within the observation time $T_{\rm obs}=2048$.

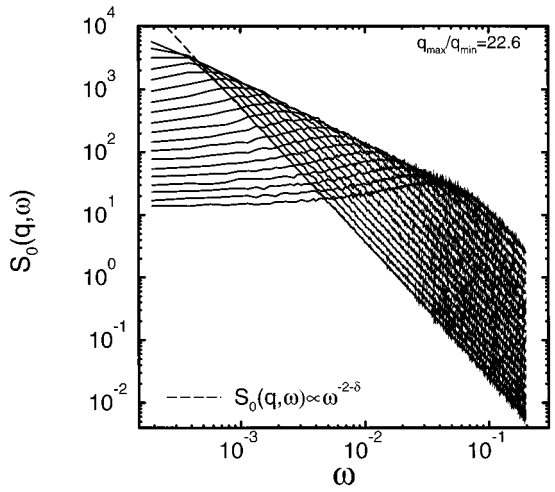


FIG. 3. Structure factor averaged over 1150 open orbits for 19 wave numbers between $q_{\min}=2\pi/800$ and $q_{\max}=22.6q_{\min}$ ($T_{\rm obs}=32768$).

which was analyzed earlier as mentioned above. Figure 8 illustrates analogous results for a lattice model.

After the ant walked for a time $t_q$ on a contour line its distance from the origin will surmount $1/q$ if the extension of its orbit is large enough. The contribution of these trajectories to the relaxation function leads to its temporal decay and, in particular, to its minimum. One obtains an estimate on $t_q$ by noting that the orbits in question for times $t<t_q$ can be considered open, so that the ant motion is superdiffusive. From Eq. (1) we infer: $t_q\propto q^{-d_h}$. Thus we conclude that the dynamical exponent $z=d_h=7/4$.

Orbits with spatial extension smaller than $1/q$, however, provide for a time independent background, as can be read off Fig. 1. This nonergodic feature of the relaxation function will be defered to Appendix A. It is absent in $F_0(\boldsymbol{q},t)$ as relaxation via open trajectories is ergodic. After subtracting this background the relaxation function is negative for times larger than $t_q$. This is a consequence of the fact that most orbits that contribute to the minimum have a tendency of trying to close on a scale not much larger than $1/q$. Thus for $t>t_q$ we observe anticorrelations rather than correlations.

For the discussion of the long time and scaling features of the density correlations we switch to the Fourier transformed

$$S(\boldsymbol{q},\omega)=\int_{-\infty}^{\infty}dt\,F(\boldsymbol{q},t)e^{i\omega t}, \tag{7}$$

which we call the structure factor. In Fig. 3 we present our data for averaging open contour lines.

From the discussion of the relaxation function the overall structure of $S(\boldsymbol{q},\omega)$ is evident immediately. In particular, for the high frequency tail we derive

$$\begin{aligned} &S(\boldsymbol{q},\omega)\propto(q/\omega)^{-2} \quad \omega\gg\omega_{\max} \\ &S_0(\boldsymbol{q},\omega)\propto(q/\omega)^{-2}\omega^{-\delta} \quad \omega\gg\omega_{\max}. \end{aligned} \tag{8}$$

From matching the high frequency behavior on the scaling form

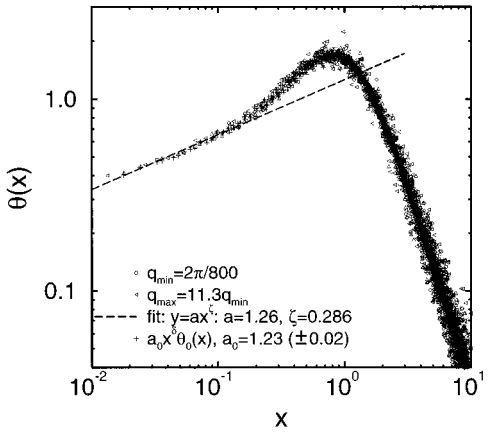


FIG. 4. Scaling function of the structure factor averaged over all 3400 detected orbits. The symbol + marks the scaling function for the open orbit average as obtained from the data in the preceding plot after rescaling according to Eq. (10).

$$\begin{aligned} &S(\boldsymbol{q},\omega)=q^{-2+\hat{\eta}}\theta(\omega/q^z), \quad z=7/4, \quad \hat{\eta}=1/2 \\ &S_0(\boldsymbol{q},\omega)=q^{-2+\hat{\eta}_0}\theta_0(\omega/q^z), \quad z=7/4, \quad \hat{\eta}_0=1/4 \end{aligned} \tag{9}$$

we find the analytical expressions for the exponents involved.

Figure 4 displays the scaling function $\theta(x)$. In our earlier paper [6] we argued that the velocity-autocorrelation functions $\Phi_0$ and $\Phi$ for the average over open and all trajectories are related: $\Phi\propto\omega^{\delta}\Phi_0$. This relation can easily be generalized

$$\theta(x)=a_0x^{\delta}\theta_0(x), \tag{10}$$

where $a_0$ is a dimensionless constant of order one. Hence, we also depict the curve $a_0x^{\delta}\theta_0$ in Fig. 4. After choosing a suitable value for $a_0$ it indeed falls onto $\theta(x)$.

The low frequency asymptotics of the scaling function we read off the same data: $\theta(x)\propto x^{\zeta}$ with $\zeta=0.28\pm0.05$. From the definition of the exponent $\eta$

$$S(\boldsymbol{q},\omega\to0)\propto q^{-2+\eta}$$

we see that the relation $\eta=\hat{\eta}-\zeta z$ holds true. Within the numerical accuracy our result for $\zeta$ suggests that

$$\eta=\eta_0=0.$$

We can observe the power law in the scaling function for a frequency interval [0.01,0.1] roughly. In the regime $\omega/q^z\ll1$, which we are interested in, the corrections to scaling are mainly due to the finite wave number. Scaling works reasonably well only for the smallest wave numbers accessible. Thus going to lower frequencies would imply the simulation of larger trajectories and, hence, much longer observation times. With the continuum method this cannot be easily achieved. For the current simulation our observation time was 327 68. This corresponds to a typical orbital radius of 1000 potential correlation lengths. Calculating a trajectory on an ALPHA 3000/400 takes roughly 30 min.

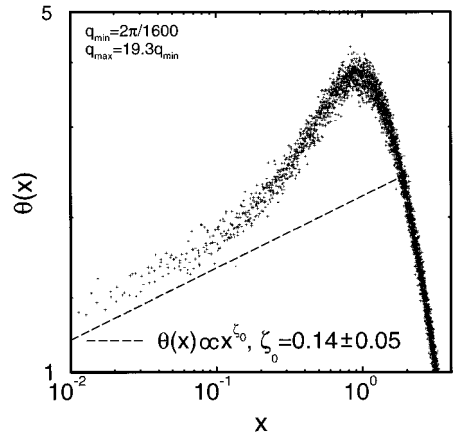


FIG. 5. Scaling function as obtained from the lattice method. The dashed line is meant as a guide to the eye. The noise present in the data is due to the lattice structure which implies the values $(-1,0,1)$ for the components of the ant's velocity vector.

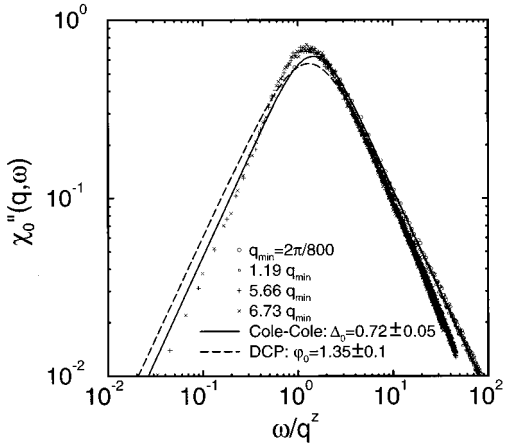


FIG. 6. Dissipative part of the complex density correlation function for four wave numbers. The solid (dashed) line represents a fit according to the Cole-Cole (diffusion coefficient) parametrization. The fit for the parameters $\Delta_0$ and $\phi_0$ orients on the high frequency tail.

**Results from a lattice method**

In a recent publication Wysokinski, Evers, and Brenig [13] have introduced an effective lattice model which captures the features of the ant paths essential for the long time dynamics without refering to the microscopic details. This model allows for the simulation of larger orbits and thus to go to lower wave numbers.

We briefly outline its central idea. The network of contour lines at a given elevation is represented by a square lattice. The nodes correspond to the saddle points in the landscape, the links to the contour lines. An ant moves along the links of the network. Each node carries an elevation $V_{sp}$, which is positive (negative) with probability ''$p$'' (''$1-p$''). At positive nodes the ant turns right, otherwise left. At the percolation threshold ''$p$'' equals 1/2.

In Fig. 5 we present the scaling function as obtained from this approach. It clearly shows the asymptotic power law.

## IV. DIFFUSION COEFFICIENT AND COLE-COLE TYPE RELAXATION

The structure factor is related to the complex density correlation function

$$\chi(\boldsymbol{q},\omega)=\chi^0(\boldsymbol{q})\frac{Dq^2}{-i\omega+Dq^2}, \tag{11}$$

as $S(\boldsymbol{q},\omega)=2\mathrm{Im}\chi(\boldsymbol{q},\omega)/\omega$, which can be considered to be an implicit definition of the diffusion constant $D$. We concentrate on averages over extended contour lines. In the foregoing we have seen that here relaxation is ergodic and thus $\chi_0^0(\boldsymbol{q})=1$, which is simply a consequence of the normalization condition

$$1=\int\frac{d\omega}{2\pi}S(\boldsymbol{q},\omega). \tag{12}$$

In order to capture the scaling structure of Eq. (9) we need to introduce a more general parametrization of $S(\boldsymbol{q},\omega)$. There are two common choices. The first one is the so called Cole-Cole form

$$\chi_0(\boldsymbol{q},\omega)=\frac{1}{1+(-i\omega\tau)^\alpha}, \tag{13}$$

$$\tau(\boldsymbol{q})=2\Delta_0(\boldsymbol{q},\omega)/q^z, \tag{14}$$

where we take $\alpha=1+\delta=8/7$ from matching on the high frequency asymptotics (8). This choice automatically respects the normalization condition if $\Delta_0$ is assumed to be constant. Note that as a consequence of the superdiffusive motion on extended contour lines $\alpha>1$.

Another parametrization which we will refer to as the diffusion coefficient parametrization (DCP) is

$$\chi_0(\boldsymbol{q},\omega)=\mathcal{N}(\delta)\frac{D_0(\boldsymbol{q},\omega)q^z}{-i\omega+D_0(\boldsymbol{q},\omega)q^z}, \tag{15}$$

$$D_0(\boldsymbol{q},\omega)=\omega^{-\delta}\varphi_0(\omega/q^z). \tag{16}$$

Again the matching procedure leads us to the scaling form for the diffusion coefficient $D_0(\boldsymbol{q},\omega)$. To consistently compare with the previous choice we assume that $\phi_0$ is simply a constant and calculate $\mathcal{N}(\delta)=1+\delta$ from the normalization condition.

In Fig. 6 we show fits for either choice of the parametrization. We have taken $\Delta_0$ and $\varphi_0$ to be constants such that the high frequency tail of the original data is reproduced. The resulting estimate of the Cole-Cole type formula for the low frequency amplitude is considerably better than the one from the DCP approach.

It is instructive to extract the diffusion coefficient $D_0$ from the data. We present our result for the scaling function $\varphi_0(x)$ in Fig. 7. Inverting the parabolic equation yields two branches which touch at a single point. We take the combination of the low frequency tail of the upper branch and the high frequency tail of the lower one as a physical solution. Clearly the deviation from the data in the DCP scheme expresses itself in a variation of the scaling function of the diffusion coefficient by a factor of 3.

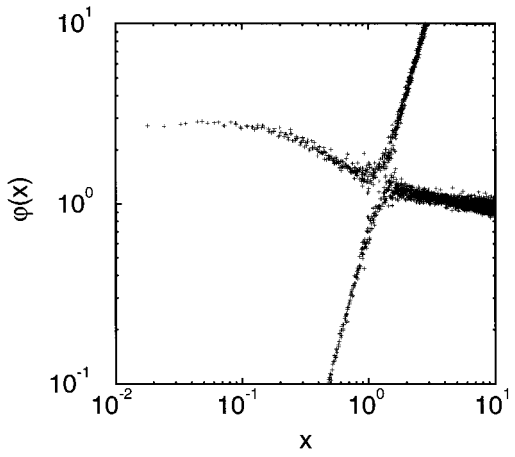


FIG. 7. Scaling function of the diffusion coefficient. The horizontal branches correspond to the physical solution of the parabolic equation. The slight negative slope at large argument is due to corrections to scaling.

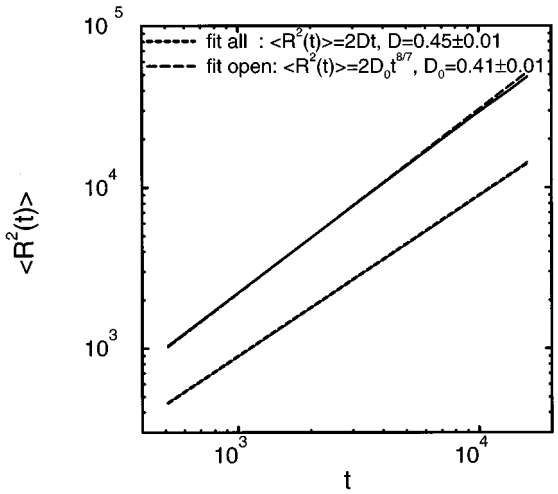


FIG. 8. Data for $\langle R^2(t)\rangle$ averaged over open (upper) and all (lower) trajectories. The total average is over 7564 of which 2190 have been open. The observation time has been 16 384 steps. (Data similar to Ref. [13], Fig. 1).

The simulation results for the total average in the scaling regime can be understood as a consequence of relation (10). We only mention that the diffusion coefficient has the structure

$$D(\boldsymbol{q},\omega)=\begin{cases} D(\omega) & \omega/\omega_{\max}\gg 1 \\ \text{const}\,\omega^{-\zeta}/q^2 & \omega/\omega_{\max}\ll 1. \end{cases} \tag{17}$$

Here $\zeta=2/7$ and $\omega_{\max}\propto q^z$ refers to the position of the maximum in the structure factor. In a previous work [6] we demonstrated that in the limit of vanishing wave number $q$, the diffusion constant $D(\omega)$ has a nontrivial frequency dependence

$$D(\omega)=D_d-\text{const}|\omega|+\cdots.$$

It leads to pronounced deviations from a perfect scaling behavior of the structure factor as can be seen, e.g., in Fig. 6.

In the current study we have concentrated on the finite $q$ behavior. For comparison with quantum calculations in the context of the quantum Hall effect it is also instructive to consider the dc conductivities in the classical models. In the lattice model the conductivity equals the diffusion constant [13], which can easily be read in Fig. 8. Here we report a more precise estimate than in a previous publication [13] which is $\sigma^c_{xx}=(0.45\pm 0.01)e^2/h$. In the continuum model the conductivity is $\sigma^c=0.5e^2/h$, independent of the microscopic parameters of the random potential [6]. As both models belong to the same universality class we conclude that the dissipative conductivity $\sigma^c_{xx}$ in the classical model cannot be a universal quantity.

## V. RELATION TO THE QUANTUM HALL EFFECT

Chalker and Daniell [14] have calculated the structure factor of wave functions for noninteracting electrons under quantum Hall conditions. They observe a similar anomaly in the diffusion coefficient Eq. (17) and the corresponding structure in the spectral scaling function $\theta_{qhe}(\omega/q^z)$. However, they find a divergency in the asymptotics of the latter at small arguments and correspondingly a negative exponent $\zeta_{qhe}=-0.19\pm 0.02$. In the opposite limit of zero wave number one obtains a well defined diffusion constant. In other numerical calculations [7,15] in the lowest Landau level the corresponding conductivity was found to be $\sigma_{xx}=0.5e^2/h$ and is supposed to be independent of microscopic details in the realization of the disorder [16]. If the quantum conductivity is indeed a universal quantity, this is in striking contrast to its classical counterpart which, according to our results, is not.

How does the different low frequency asymptotics in the scaling function for the classical contour line approach and the wave function calculations come about? First we discuss the average over extended trajectories. As contour lines never intersect (except for the possibility of touching at a saddle point) they constitute a special kind of self-avoiding random walk. In particular, if the ant has been at a place some time $t$ ago and wants to go back, it has to find a path which does not cross the path defined by the steps taken at times earlier than $t$. With increasing $t$ this becomes more and more difficult. In other words, ants have difficulties, after leaving a certain area, returning to their origin. Thus in the sector of $\omega/q^z\ll 1$ density fluctuations are suppressed.

If we average over all paths these considerations still apply. However, the fraction of large orbits having small frequency components in the relaxation function is reduced, so that $S(\boldsymbol{q},\omega)$ decays faster than $S_0(\boldsymbol{q},\omega)$. The trajectories smaller than $1/q$ lead to the $\delta(\omega)$ spike in $S(\boldsymbol{q},\omega)$ which we treat in Appendix A.

We believe that the different features of the structure factors at criticallity and low frequency are due to the possibility of tunneling in a wave function picture. Interference effects present in quantum mechanical calculations, coupled to potential disorder, lead to pronounced resonances. If the potential fluctuations are sufficiently strong and of long range these can support even (quasi-) classical substructures in the wave function [17]. In the classical contour line approach there is a fast decay channel for the density correlations via transport along the classical trajectories. We speculate that a similar fast channel also is present in the quantum system.

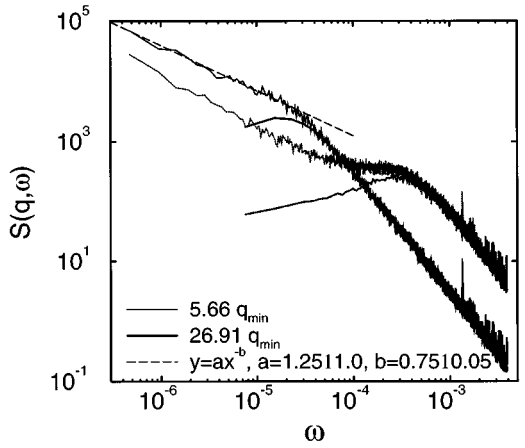


FIG. 9. Structure factor for ''hopping''ants (diverging curves at $\omega\to 0, T_{\rm obs}=209\,715\,2$, W=200) and ''nonhopping'' ants ($T_{\rm obs}=131\,072$, W=$\infty$) for two different wave numbers ($q_{\rm min}=2\pi/1600$).

However, in addition there is a possibility for the slower decay of sharp resonances. This provides the main amplitude in the $\omega/q^z \ll 1$ section of the structure factor. If corresponding classical orbits exist—as in the case of strong, long ranged random potentials—these are inert and caught in the $\delta(\omega)$ peak of $S(\boldsymbol{q},\omega)$.

Figure 9 further illustrates this point. The data curves diverging at zero frequency are obtained from a slightly modified version of the lattice model [17] constituting a ''weakly self-avoiding random walk.'' We have destablized the closed ant paths by allowing the ant to move left (right) with a probability $T\propto e^{-V_{sp}}$ (or $1-T$, respectively) even at positive (negative) nodes. The elevations we pick from a homogenous distribution $[-W,W]$. This ''ant hopping'' is meant as a crude caricature of the actual resonance decay. It comes with a power law divergency in the low frequency section which is produced by a broad distribution of decay times of the originally stable classical orbits. Of course, our oversimplified model does not properly account for the complicated multifractal structure of the wave function [18] and the corresponding decay statistics. So $\eta'=0.75\pm 0.05$ turns out to be twice as large as the correct value $\eta=0.38\pm 0.04$.

## VI. SUMMARY

We have simulated the density correlation function for directed propagation on contour lines in a random landscape at criticality. The structure factor is of a scaling form but has a special feature in that the scaling function vanishes at small arguments. This anomaly is a consequence of the superdiffusive motion on extended contour lines inherently described by the fractal dimension of the hull $d_h$. Under the assumption that the scaling function of the diffusion coefficient obtained when averaging extended contour lines can be approximated by a constant number, the anomaly can qualitatively be understood. Furthermore, all scaling exponents can be traced back to $d_h$. In particular, we find $\eta=0$. The anomaly changes its character completely if one allows for the hopping of ants walking on a closed contour line across saddle points to other lines. In this case the structure factor diverges with a power law, reminiscent to a similar anomaly in the quantum Hall effect. However, whereas here the conductivity is believed to be a universal quantity, our calculations show that it is not universal in the classical models.

## ACKNOWLEDGMENTS

During the course of this work I have appreciated valuable discussions with Dietrich Belitz, Berndt Gammel, Rochus Klesse, Peter Kratzer, Rajesh Narayanan, Thomas Vojta, and, in particular, with Wilhelm Brenig and Karol Wysokinski. I am grateful to all of them. This work was supported by the NSF under Grant No. DMR-95-10185.

## APPENDIX A: RELAXATION FUNCTION AT ZERO FREQUENCY

The contribution of closed orbits with a spatial extension smaller than $1/q$ inhibits the relaxation of density fluctuations back into the homogenous equilibrium state. Consequently the decay of the relaxation function

$$F(\boldsymbol{q},t)=\langle\cos\{\boldsymbol{q}[\boldsymbol{r}(t)-\boldsymbol{r}(0)]\}\rangle$$

is not completely down to zero. Instead it attains a finite number even at very large times

$$\lim_{t\to\infty} F(\boldsymbol{q},t)=1-f(\boldsymbol{q}). \tag{A1}$$

Here as a consequence of the normalization condition (12) the nonergodicity parameter $f(\boldsymbol{q})$ is related to the quasistatic, isolated susceptibility $\chi^0(\boldsymbol{q})$. One can easily determine how $f(\boldsymbol{q})$ must depend on its argument: The contribution of orbits much smaller than $1/q$ to the average in Eq. (5) is 1. This implies that $1-f(\boldsymbol{q})$ is the ratio of all contour lines smaller than $1/q$ or equivalently that $f(\boldsymbol{q})$ is the ratio of orbits larger than $1/q$. It is straightforward to derive from analogy to percolation theory that the fraction of lines with length larger than $L$ obey a power law with an exponent $-1/7$ [6]. The fractal dimension of the hull $d_h$ relates the length of a contour line to its spatial extension: $R^{d_h}\propto L$. Taking all the information together we conclude

$$f(\boldsymbol{q})\propto q^{1/4}. \tag{A2}$$

This is in good agreement with our numerical data shown in Fig. 10.

So far we have discussed the relaxation function only. As a consequence of its nonergodic character the full structure of the spectral function is

$$S(\boldsymbol{q},\omega)=2\pi[1-f(\boldsymbol{q})]\delta(\omega)+\tilde{S}(\boldsymbol{q},\omega), \tag{A3}$$

where $\tilde{S}(\boldsymbol{q},\omega\to 0)=0$.

## APPENDIX B: SLOWING DOWN AT SADDLE POINTS

Consider an ant moving on an infinitely extended trajectory. During its walk it comes close to certain saddle points along its path. At these particular instances the velocity of the ant becomes very small. More precisely, for a given tiny velocity, we can always observe the ant approaching a saddle

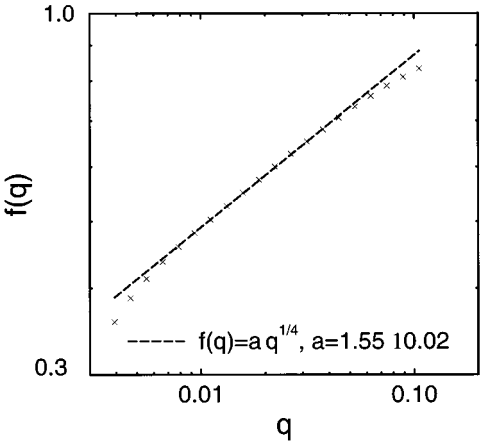


FIG. 10. Wave number dependence of the nonergodicity parameter $f(\boldsymbol{q})$.

point where its speed is even smaller than the given one, provided that we wait for a sufficiently large amount of time. Thus one concludes that the average ant velocity we measure should depend on the observation time: the longer we observe, the lower the mean value $\overline{v}$ will be. This effect is of relevance for our analysis of the long time dynamics of the ants if $\overline{v}$ vanishes in the limit of infinite observation time. In this appendix we demonstrate that slowing down at critical saddle points is an effect too weak to diminish the ants mean velocity considerably.

Near the saddle points of interest to us the potential can be parametrized in a parabolic approximation

$$V(x,y)=V_{sp}-(a/2)x^2+(b/2)y^2.$$

As the ant moves at constant elevation its position $(X,Y)$ can be parametrized by a single coordinate, say $X$. We integrate the equations of motion (3) to find the time $t_{i0}$ needed for the ant to walk from some spot $X_i$ near the saddle point to the position $X_0$ where its distance is minimal

$$t_{i0}(X_0)=\frac{1}{\sqrt{ab}}\ln\left(\frac{X_i+\sqrt{X_i^2-X_0^2}}{X_0}\right). \tag{B1}$$

An ant heading straight to the saddle point (corresponding to $X_0=0$) would need a logarithmically infinite time to actually get there and thus stop altogether.

Next we estimate the impact of this effect on the mean velocity measured on a piece of a contour line of length $L$. When traveling the ant passes $Z_L(X_0)$ saddle points located a distance $X_0$ from its path. A measure for the time $T_{i0}$ spend near these locations is

$$T_{i0}=\int_0 dX_0 Z_L(X_0)t_{i0}(X_0).$$

Introducing the distribution function

$$P(X_0)=\lim_{L\to\infty} Z_L(X_0)/L$$

and the total time $T_\Delta$ spend for traveling in between the saddle points we define a mean velocity $\overline{v}$

$$\overline{v}^{-1}=\frac{T_\Delta+T_{i0}}{L}=\left(T_\Delta+\int_0 dX_0 P(X_0)t_{i0}(X_0)\right)\Big/ L.$$

In a numerical study we found that $P(X_0)$ vanishes linearly at small arguments. Thus it completely suppresses the weak logarithmic divergency of $t_{i0}$ in the integrand and the mean velocity is finite. We did an independent check on this result by investigating the mean velocity of ants living on closed orbits as a function of the length of this orbit. We found $\overline{v}(L)=0.96$ essentially independent of $L$. Thus we conclude that assuming a finite mean velocity for the traveling ants independent of their orbital extension is very well justified and slowing down near saddle points can safely be ignored for our purposes.

[1] R. Zallen and H. Scher, Phys. Rev. B **4**, 4471 (1971).
[2] A. Weinrib and S. A. Trugman, Phys. Rev. B **31**, 2993 (1985).
[3] R. Kubo, S. J. Miyake, and N. Hashitsume, in *Solid State Physics*, edited by F. Seitz and F. Turnbull (Academic, New York, 1965).
[4] M. Tsukada, J. Phys. Soc. Jpn. **41**, 1466 (1976); S. A. Trugman, Phys. Rev. B **27**, 7539 (1983); R. Mehr and A. Aharony, *ibid.* **37**, 6349 (1988).
[5] S. Koch, R. J. Haug, K. von Klitzing, and K. Ploog, Phys. Rev. Lett. **67**, 883 (1991).
[6] F. Evers and W. Brenig, Z. Phys. B **94**, 155 (1994).
[7] B. M. Gammel and W. Brenig, Phys. Rev. B **53**, 13 279 (1996).
[8] P. Kratzer and W. Brenig, Z. Phys. B **94**, 147 (1994).
[9] M. Hund, Physica A **175**, 239 (1991).
[10] M. B. Isichenko, Rev. Mod. Phys. **64**, 961 (1992).
[11] S. Fujiwara and F. Yonezawa, Phys. Rev. Lett. **74**, 4229 (1994).
[12] H. L. Zhao and S. Feng, Phys. Rev. Lett. **70**, 4134 (1993).
[13] K. I. Wysokinski, F. Evers, and W. Brenig, Phys. Rev. B **54**, 10 720 (1996).
[14] J. T. Chalker and G. J. Daniell, Phys. Rev. Lett. **61**, 593 (1988).
[15] Y. Huo, R. E. Hetzel, and R. N. Bhatt, Phys. Rev. Lett. **70**, 481 (1993).
[16] I. M. Ruzin, N. R. Cooper, and B. I. Halperin, Phys. Rev. B **53**, 1558 (1995).
[17] F. Evers and W. Brenig (unpublished).
[18] M. Janssen, O. Viehweger, U. Fastenrath, and J. Hajdu, *Introduction to the Theory of the Integer Quantum Hall Effect*, edited by J. Hajdu (VCH, Weinheim, 1994).